

NUCLEOSYNTHETIC ANOMALIES IN PALLADIUM FROM BULK METEORITES. B. Mayer¹ and M. Humayun¹, ¹National High Magnetic Field Laboratory & Dept. of Earth, Ocean & Atmospheric Science, Florida State University, Tallahassee, FL 32310, USA (mayer@magnet.fsu.edu)

Introduction: Solar system materials exhibit nucleosynthetic anomalies in Sr, Zr, Mo, Ru, and Ba from bulk chondrites, calcium aluminum inclusions (CAI), and irons [1-7]. Isotope anomalies are more limited in W [8-10] or absent in Os [10-11]. The origin of these anomalies is still highly debated and may represent spatial and/or temporal heterogeneity in the sources that supplied material to the nascent solar nebula, and/or may have been enhanced by chemical processing within the solar nebula [e.g. 12-14]. In comparison to the elements which have been investigated previously, the siderophile element Pd is not refractory during nebular processing with similar condensation temperature as the Fe peak elements (e.g. Fe, Ni). Thus, Pd is important for testing hypotheses which invoke variable degrees of homogenization of nucleosynthetic anomalies for different elements. We have previously reported Pd isotopic compositions of IVB iron meteorites [15] that demonstrated distinct nucleosynthetic anomalies in $\epsilon^{104}\text{Pd}$ and $\epsilon^{110}\text{Pd}$. Here, we present new Pd isotope ratio measurements of chondrites and iron meteorites to extend our previous work.

Analytical Methodology: Samples from 5 chondrites (3 H, 1 CB and 1 CV), and 3 IAB, 4 IIAB, 4 IIIAB, 5 IVA and 10 IVB iron meteorites were freshly cut and polished, then dissolved in aqua regia and HF:HNO₃. The matrix and elements that create isobaric interferences (Zn, Zr, Mo, Ru, Cd etc.) were removed with cation and anion exchange column chemistry [15]. All Pd-isotopic compositions were analyzed on a Thermo Neptune™ MC-ICP-MS in medium resolution and static mode in 100 ng/mL Pd aliquots in 2% HCl introduced with an ESI APEX™ sample introduction system or Cetac Aridus II desolvating system. Thermo SuperJet8.2 Ni and Spectron T1001 Ni-X skimmer cones were used. Mass bias correction was performed with the exponential law with ratios normalized to $^{108}\text{Pd}/^{105}\text{Pd} = 1.18899$. All data are given in epsilon notation as deviation from the terrestrial reference material, a Pd High Purity Standard™. Possible minor isobaric interferences from Ru (^{101}Ru) and Cd (^{111}Cd) were simultaneously monitored on the MC-ICP-MS. To establish the purity of the Pd cuts and to monitor possible interferences, all samples were analyzed with an ICP-MS (Thermo Element2™ or Element XR™) prior to measurement on the MC-ICP-MS. **Results:** New results are shown in Figs. 1 and 2. Relative to the terrestrial Pd standard, Pd isotopic anomalies are clearly seen in all meteorites except for IAB

iron meteorites and H chondrites. For all samples, the Pt isotopic composition on the same aliquot has been measured and used as an *in situ* dosimeter [8, 10] for galactic cosmic ray (GCR) damage (see discussion below). For all samples which exhibit a positive anomaly in $\epsilon^{110}\text{Pd}$ a corresponding negative anomaly is resolved after GCR correction in $\epsilon^{104}\text{Pd}$.

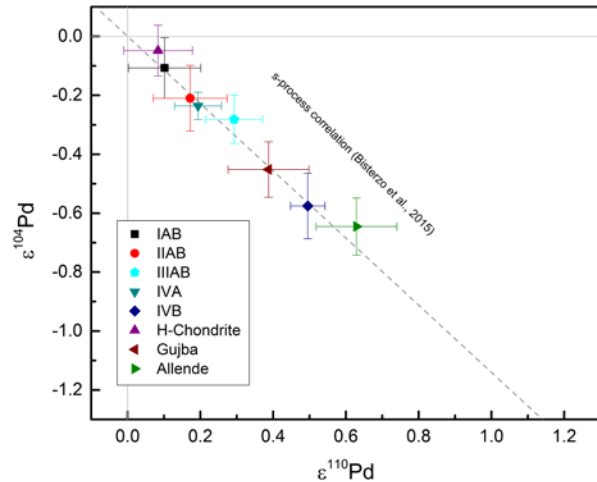


Fig. 1: Pd isotopic composition of chondrites and iron meteorites with $2\sigma_{\text{mean}}$ errors. Note that $\epsilon^{104}\text{Pd}$ and $\epsilon^{110}\text{Pd}$ (minor corrections) are GCR corrected. The black line corresponds to an s-process deficit obtained by subtracting the s-process yields [17] from a reservoir with terrestrial isotopic composition.

Discussion: Cosmogenic effects. Cosmogenic neutron capture on ^{103}Rh results in an excess in ^{104}Pd with minor burning of ^{105}Pd and ^{108}Pd , while the r-process only isotope ^{110}Pd has limited to no cosmogenic effects. The variable anomalies in $\epsilon^{104}\text{Pd}$ within each iron group are well correlated with the *in situ* neutron dosimeter based on $\epsilon^{192}\text{Pt}$ [8, 10, 15, 16]. Due to the low Ir/Pt in Grant (IIIAB) corrections with $\epsilon^{192}\text{Pt}$ or $\epsilon^{196}\text{Pt}$ result in similar propagated errors on the $\epsilon^{104}\text{Pd}$. After GCR corrections, all iron meteorites (Fig.1) exhibit a resolved anomaly in $\epsilon^{104}\text{Pd}$ and $\epsilon^{110}\text{Pd}$ (except for IAB iron meteorites).

Nucleosynthetic effects. In Figs. 1-3, the expected s-process deficits are modeled by subtracting the s-process yields [18] from solar abundances. The slope of the s-process line is not affected by using different input parameters (e.g. single vs. main AGB star abundances, Galactic Chemical Evolution model, different MACS; see discussion in [15]). Fig. 1 shows that $\epsilon^{104}\text{Pd}$ anomalies in chondrites and iron meteorites anticorrelate with the $\epsilon^{110}\text{Pd}$ anomaly exactly as for an s-process deficit (Fig. 1). Similar nucleosynthetic anomalies in these meteorites are also observed in oth-

er elements, like Sr, Zr, Ru, Mo, Ba and W [1-10] (Fig. 2-3) but not found in Os [10, 11]. An s-process deficit model works well to explain correlated Ru-Mo nucleosynthetic anomalies, and this deficit may be carried by a single presolar phase, e.g., SiC [4, 12].

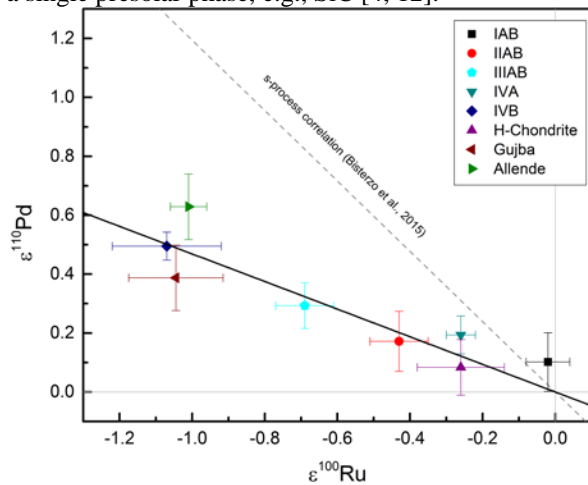


Fig. 2: Pd and Ru [5, 6] isotopic compositions of chondrites and iron meteorites. Black dashed line [17] same as in Fig. 1.

If a single carrier phase, or set of phases, was the host for Pd this would have yielded a similar correlation for Ru-Pd (Fig. 2). However, Pd shows significantly lower anomalies than Ru (Fig. 2) or Mo for both chondrites and iron meteorites, so that the simple model fails to account for the Pd isotopes. Late injection of supernova material [14] also does not produce the Pd-Ru correlation. In Fig. 3, this observation is extended to a larger set of elements where isotope anomalies in Zr, Mo and Ru show similar magnitudes of s-process deficit in both iron meteorites and chondrites, while Pd and Ba both show about half that magnitude. Since Pd has a lower condensation temperature than Zr, Mo or Ru, thermal processing of the presolar carriers might yield the observed correlation. A thermal process could enhance the Zr, Mo, and Ru anomalies while still preserving a correlation between Ru, Mo, and Pd only if it operated uniformly on carriers in both irons and chondrites. An alternative possibility is that a carrier without Pd (e.g., SiC) which exhibits s-process excess in Zr, Mo and Ru [18,19] was mixed with the thermally processed carrier(s). To preserve the observed correlation between Ru and Pd, the ratio of these two carrier populations would have to be very similar. Among the refractory elements, Ba is the most likely to be affected by volatility, especially under oxidizing conditions [20]. The fact that Ba anomalies are similar in magnitude to Pd anomalies in Allende [7] supports the idea that isotope anomalies are the relicts of thermal processing and partial homogenization within the solar nebula. The thermal (and physical) processing of chemically diverse presolar carriers and the resulting

anomalies must have occurred prior to the formation of the iron meteorite parent bodies and chondrites, i.e. <1 Ma after CAIs. This study reveals that the distribution of Pd nucleosynthetic anomalies in meteorites is vital to clarify the nature, origin, and development of the observed nucleosynthetic anomalies in the early solar system. It also explains why nucleosynthetic anomalies are rare or absent from volatile elements [e.g. 21,22].

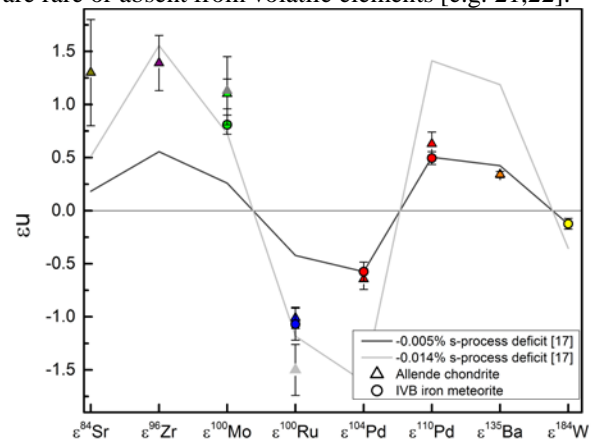


Fig. 3: Comparison between Sr [1] dark yellow, Zr [2] purple, Mo [3] grey, [4] green, Ru [5], grey, [6] blue, Pd (red), Ba [7] orange, and W [8] yellow isotopic anomalies in IVB iron meteorites (circle) and Allende (square). For guidance two s-process deficit lines with different deficits are shown (dark grey: -0.005% forced through Pd, Ba, and W and light grey: -0.014% forced through Mo and Ru for IVB measurements).

References: [1] Brennecka, G. et al. (2013) PNAS, 110, 17241-17247. [2] Akram, W. et al. (2015) GCA, 165, 484-500. [3] Dauphas et al. (2002) ApJ, 565, 640-644. [4] Burkhardt, C. et al. (2011) EPSL, 312, 390-400. [5] Chen, N. et al. (2010) GCA, 74, 3815-3862. [6] Fischer-Gödde, M. et al. (2015) GCA, 168, 151-171. [7] Bermingham, K. et al. (2015) GCA, 175, 282-298. [8] Kruijer T. et al. (2013) EPSL 361, 162-172. [9] Markowski, A. et al. (2006) EPSL, 242, 1-15. [10] Wittig, N. et al. (2013) EPSL, 361, 152-161. [11] Walker, R. J. (2012) EPSL, 315-352, 36-44. [12] Dauphas N. et al. (2004) EPSL 226, 465-475. [13] Trinquier, A. et al. (2009) Science, 324, 374-376. [14] Vanhala, H. & Boss, A. (2001) ApJ, 575, 1144-1150 [15] Mayer, B. et al. (2015) ApJ, 809, 180. [16] Leya, I. & Masarik, J. (2013) Science, 48, 665-685. [17] Bisterzo, S. et al. (2015) MNRAS, 449, 506-527. [18] Savina, M. et al. (2004), Science, 303, 649-652. [19] Nicolussi, G. et al. (1998) ApJ, 504, 492-499. [20] Davis, A.M. et al (1982) GCA, 46, 1627-1651 [21] Moynier, F. et al. (2007) GCA, 71, 4365-4379. [22] Wombacher, F. et al. (2008) GCA, 72, 646-667.